REANALYSIS OF MARS ORBITER LASER ALTIMETER ATMOSPHERIC FEATURES WITH MACHINE LEARNING ALGORITHMS.

V. Caillé, *LATMOS, Sorbonne Université, UVSQ Paris-Saclay, CNRS, Paris, France (vincent.caille@latmos.ipsl.fr)*, **A. Määttänen,** *LATMOS, Sorbonne Université, UVSQ Paris-Saclay, CNRS, Paris, France*, **A. Spiga,** *LMD/IPSL, Sorbonne Université, Paris, France - Institut Universitaire de France, France*, **L. Falletti,** *LATMOS, Sorbonne Université, UVSQ Paris-Saclay, CNRS, Paris, France*, **G. A. Neumann,** *NASA Goddard Space Flight Center, Greenbelt, Maryland, USA*.

Introduction

The Martian atmosphere is a mix of diverse kinds of aerosols structures and clouds with different compositions such as dust, water or CO_2 ice. Processes involved in their formations are complex and their understanding have been enhanced by observations from the last decades mission. Between 1996 and 2006, Mars Global Surveyor (MGS) carried three instruments, the Mars Orbiter Camera (MOC), the Thermal Emission Spectrometer (TES) and the Mars Orbiter Laser Altimeter (MOLA) that have all been able to observe clouds during the same period with different methods. Gathering and comparing results from these three datasets could give an appreciation of what has happened in the Martian atmosphere during 1,5 martian years. However, previous studies of MOLA observations of clouds [Neumann et al., 2003, Ivanov and Muhleman, 2001] were numerically restrained and we suggest that reanalysing the dataset with recent methods could give more clouds and dust observations. Since then, both MOC and TES datasets have also been analysed, allowing us to compare all three instruments observations. We could also compare our results with observations from missions launched after MGS and modeling results.

MOLA [Zuber et al., 1992] was an altimeter aboard MGS which first goals were to draw precise Mars topography, roughness and albedo at 1064 μm-wavelength maps using a pulsing laser directed towards Mars' surface [Smith et al., 2001]. Nevertheless, martian clouds were dense enough to trigger MOLA receptor and previous studies showed that some laser returns were signatures of atmospheric features. Their distinction of the different kinds of returns (surface, noise or atmospheric features) have been made using stringent detection criteria to deal with the consequent amount of data. Thought it ensured that there were as few false positives as possible in their atmospheric features observations, it eventually led to missing an important part of them.

Method & Validation

Machine learning algorithms, and especially clustering methods are an interesting way to extract specific features from massive dataset. K-means method is usually a good first approach for analysing dataset with such methods because it is certain to converge [Selim and Ismail, 1984] and quickly enough [Har-Peled and Sadri, 2004]. In order to apply it to MOLA dataset, we first have to optimize both the distinguishing variables and the desired number of clusters k. Following [Neumann et al., 2003] work, the product of surface reflectivity with the two-way atmosphere transmissivity, rT^2, can be used as a returned laser energy, normalised by MOLA performances over the mission duration and has a clear signature for atmospheric returns when plotted against time : while surface returns form a continuum and noise returns are sporadic sudden variations, atmospheric features returns cause a dip lasting for several consecutive returns. Three independent methods, elbow, silhouette score and gap statistic, allow to get the optimised number of clusters by evaluating the clustering performances for different k. It allowed us to see that both $k = 5$ and $k = 6$ had similar performances but we decided to go for $k = 6$ because it eased interpretation of each cluster and lowered the chance of getting false positives in our atmospheric features cluster. We subsequently applied K-means method to all 12 mission orbital phases. Clustering results (example given for one orbital phase in figure 1) present the expected clusters, and especially one made of atmospheric features returns.

Validation of our distinction method results is made by comparing our atmospheric features seasonal and latitudinal distribution (fig 2) with the ones obtained in reference study [Neumann et al., 2003]. Areas or seasons with the highest density of atmospheric returns, like north pole during northern autumn, cloudy episode between 30°S and 60° at the end of southern winter or the almost global coverage around L_s 230° are present in both distributions and show that our results are in total agreement with previous results. However, we end up having almost 33 times more atmospheric returns. We regrouped consecutive atmospheric returns into atmospheric structures, that can be dust, water or CO_2 ice clouds and saved them into a catalog in order to ease their visualisations.

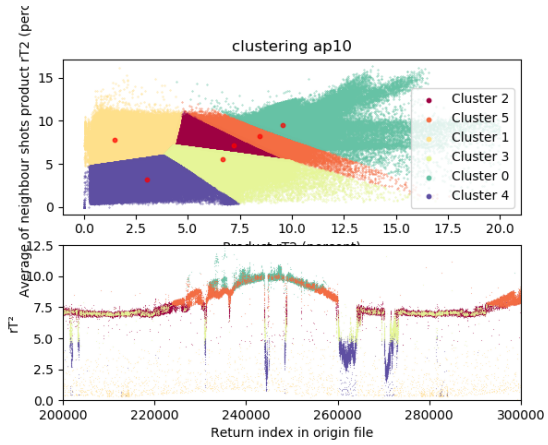

Figure 1: Clustering structure for one orbital phase (top) and example of an atmospheric feature in rT^2 against time plot (bottom)

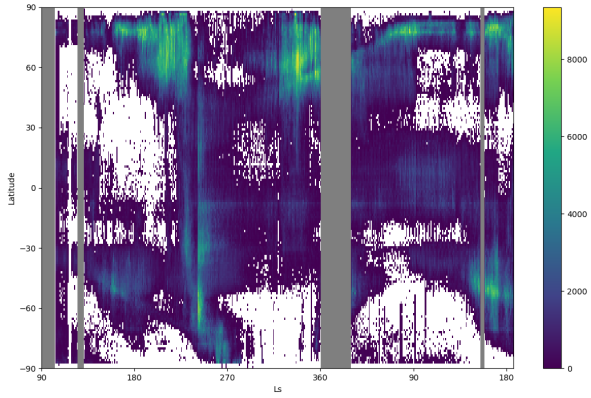

Figure 2: Seasonal and latitudinal distribution of atmospheric features, colors represent number of returns in 1°x1° bin around each point

Atmospheric Features Variability & Diversity

We divided the dataset into windows of 15° of solar longitude to draw maps of longitudinal and latitudinal distribution of atmospheric features during the whole mission. This gives a final results of what could be observed in the low altitude atmosphere by MOLA during MY24 from L_s 103° (fig 3) and the first half of MY25 till L_s 187° (fig 4) and allow us to analyse interannual variability as well as seasonal variability. By comparing the only period we have in common for both years, ie southern winter, we can see that there were way more atmospheric structures during MY25. However, their distributions are very similar for both years, apart from Tharsis Montes where big structures (at least 150 km long) only formed during MY25. These big structures distribution do not follow the global distribution (fig 2), what highlights some areas of interest such as Hellas Basin, Valles Marineris, Syrtis Major...

These maps also allow to see some well-known phenomenon that occur in the Martian atmosphere that were not observed that well by MOLA previously. By combining results from both years, every stages of the aphelion cloud belt can be seen, from its formation around L_s 15-30° till its density peak around L_s 120°. Even if MOLA analysis does not provide us any information about atmospheric structures compositions, comparison with TES [Hale et al., 2011] and MOC [Wang and Ingersoll, 2002] observations allow us to determine that most of these clouds are water clouds. The development of the south polar hood and its correlation with the decline of the south polar cap toward the south pole during southern spring can also be observed while being absent in MOC observations, what is coherent with assumptions of these structures being CO_2 ice clouds. We are also coherent with global climate model dust profiles that established an almost global coverage between L_s 220° and L_s 260° during MY24 [Montabone et al., 2015], what is observed in our results. Formation and evolution of clouds above the poles are also analysed and linked to other missions observations.

Acknowledgements

We thank the Agence National de la Recherche for funding (projet MECCOM, ANR-18-CE31-0013). This work was performed using HPC computing resources from GENCI-CINES (Grant 2021-A0100110391), and resources at the ESPRI mesocentre of the IPSL institute

Figures

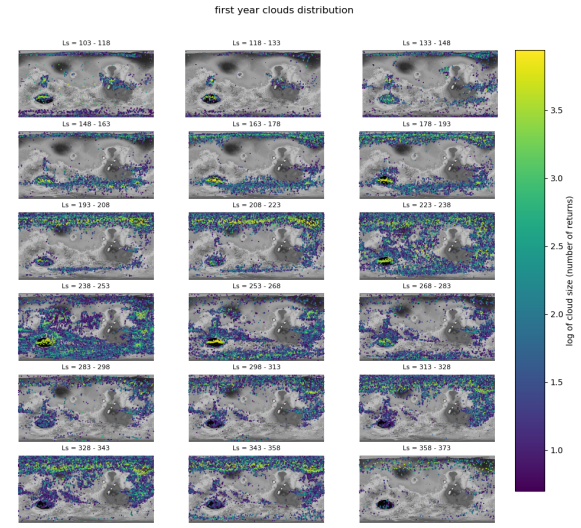

Figure 3: 15° longitudinal and latitudinal maps of atmospheric features during MY24. Colorbar represents the size of atmospheric structures in log-scale

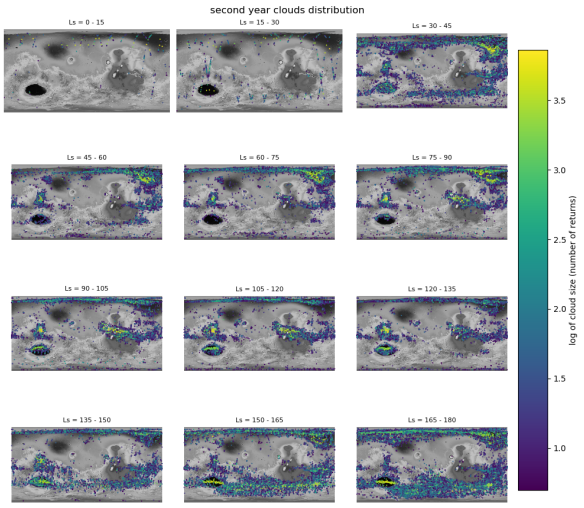

Figure 4: 15° longitudinal and latitudinal maps of atmospheric features during MY25. Colorbar represents the size of atmospheric structures in log-scale

References

[Hale et al., 2011] Hale, A., Tamppari, L., Bass, D., and Smith, M. (2011). Martian water ice clouds: A view from mars global surveyor thermal emission spectrometer. *Journal of Geophysical Research*, 116.

[Har-Peled and Sadri, 2004] Har-Peled, S. and Sadri, B. (2004). How fast is the k-means method? *Algorithmica*, 41(3):185â202.

[Ivanov and Muhleman, 2001] Ivanov, A. B. and Muhleman, D. O. (2001). Cloud reflection observations: Results from the mars orbiter laser altimeter. *Icarus*, 154(1):190–206.

[Montabone et al., 2015] Montabone, L., Forget, F., Millour, E., Wilson, R., Lewis, S., Cantor, B., Kass, D., KleinbÃ¶hl, A., Lemmon, M., Smith, M., and et al. (2015). Eight-year climatology of dust optical depth on mars. *Icarus*, 251:65â95.

[Neumann et al., 2003] Neumann, G. A., Smith, D. E., and Zuber, M. T. (2003). Two Mars years of clouds detected by the Mars Orbiter Laser Altimeter. *Journal of Geophysical Research (Planets)*, 108(E4):5023.

[Selim and Ismail, 1984] Selim, S. Z. and Ismail, M. A. (1984). K-means-type algorithms: A generalized convergence theorem and characterization of local optimality. *IEEE Transactions on Pattern Analysis and Machine Intelligence*, PAMI-6(1):81–87.

[Smith et al., 2001] Smith, D. E., Zuber, M. T., Frey, H. V., Garvin, J. B., Head, J. W., Muhleman, D. O., Pettengill, G. H., Phillips, R. J., Solomon, S. C., Zwally, H. J., Banerdt, W. B., Duxbury, T. C., Golombek, M. P., Lemoine, F. G., Neumann, G. A., Rowlands, D. D., Aharonson, O., Ford, P. G., Ivanov, A. B., Johnson, C. L., McGovern, P. J., Abshire, J. B., Afzal, R. S., and Sun, X. (2001). Mars orbiter laser altimeter: Experiment summary after the first year of global mapping of mars. *Journal of Geophysical Research: Planets*, 106(E10):23689–23722.

[Wang and Ingersoll, 2002] Wang, H. and Ingersoll, A. P. (2002). Martian clouds observed by mars global surveyor mars orbiter camera. *Journal of Geophysical Research: Planets*, 107(E10):8–1–8–16.

[Zuber et al., 1992] Zuber, M. T., Smith, D. E., Solomon, S. C., Muhleman, D. O., Head, J. W., Garvin, J. B., Abshire, J. B., and Bufton, J. L. (1992). The mars observer laser altimeter investigation. *Journal of Geophysical Research: Planets*, 97(E5):7781–7797.